J. Appl. Comput. Mech., 12(2) (2026) 632-647
DOI: 10.22055/jacm.2025.48506.5285

ISSN: 2383-4536
jacm.scu.ac.ir

Shahid Chamran
University of Ahvaz

Journal of
Applied and Computational Mechanics

Research Paper

Semi-Analytic Scheme for Fractional Insight into Multi-Component KdV System Arises in Water Wave Mechanism

Shelly Arora[1], Wen Xiu Ma[2,3,4,5], Sukhjit Singh Dhaliwal[6], Atul Pasrija[1]

[1] Department of Mathematics, Punjabi University, Patiala, 147002, India, Email: aroshelly@pbi.ac.in (S.A.); atulpasrija_rs@pbi.ac.in (A.P.)

[2] Department of Mathematics, Zhejiang Normal University, Jinhua, 321004, Zhejiang, PR China, Email: mawx@cas.usf.edu

[3] Department of Mathematics, King Abdulaziz University, Jeddah, 21589, Saudi Arabia

[4] Department of Mathematics and Statistics, University of South Florida, Tampa, 33620-5700, USA

[5] Material Science Innovation and Modelling, Department of Mathematical sciences, North-West University, Mafikeng Campus, Mmabatho, 2735, South Africa

[6] Department of Mathematics, SLIET, Longowal, Sangrur, 148106, Punjab, India, Email: sukhjit_d@sliet.ac.in

Received June 05 2025; Revised August 13 2025; Accepted for publication September 05 2025.
✉ Corresponding authors: W.X. Ma (mawx@cas.usf.edu); A. Pasrija (atulpasrija_rs@pbi.ac.in)

Abstract. The present study aims to broaden the applications of a newly emerged Laplace-like transform known as the generalized bivariate integral transform. This transform is combined with the homotopy perturbation method to obtain approximate and analytic solutions for the fractional multi-component Korteweg-de Vries system. The time fractional derivative is considered in the conformable sense. The scheme involves the applications of generalized bivariate transform and its inversion to handle fractional operator. He's polynomials, associated with homotopy perturbation method, are employed to decompose the non-linearity of the proposed problem. Through the combination of these two powerful tools, an iterative expression is derived to compute the components of a rapidly convergent series solution. A rigorous analysis is conducted, and sufficient conditions for convergence are presented in detail. The proposed procedure effectively demonstrates distinct soliton mechanisms under various of initial conditions for proposed fractional system. The novelty of this study lies in the first-time application of the proposed scheme to a conformable fractional system. A key highlight of the study is the convergence behavior for non-integer order derivatives to study soliton behavior even in the absence of a known exact solution.

Keywords: Generalized bivariate transform, Homotopy perturbation method, Semi-analytic scheme, KdV-system, Conformable fractional derivative.

1. Introduction

Fractional calculus initially emerged in the correspondence between Leibniz and L' Hospital concerning the definition of d^n / dx^n for $n = 1/2$ in 1695. It deals with the arbitrary order of differential and integral operators. The fractional differential equation captures hereditary and memory-based dynamics through its distinctive non-local essence. The physical description of several natural processes via fractional differential equations is found with greater precision than integer-order differential equations. These include solitary waves, signal and image processing, Levy statistics, material science, turbulence, porous media, wrinkled frame front propagation, and anomalous diffusion. The immense applicability of fractional equations motivates a considerable level of activeness in understanding and predicting the behavior of non-linear equations modeled in a fractional framework. For fractional derivatives, there are innumerable operators: Riemann-Liouville (R-L), Liouville-Caputo (L-C), Caputo-Fabrizio (C-F), and Atangana-Baleanu-Caputo (ABC), respectively, which are associated with power laws, exponential decay laws, and generalized Mittag Leffler functions [1-3]. Fractional initial conditions are physically inconsistent in the R-L formulation. On the other hand, the initial conditions described in terms of integer-order derivatives signify the physical interpretation in the L-C formulation. The complications of singular kernel and its applicability to only differentiable functions limit the scope of the L-C operator. In order to assist with non-local and non-singular kernel properties, C-F and ABC are defined as extensions of the L-C operator. But using a non-singular fractional differential operator has several setbacks. Diethelm [4] reported the failure of a fractional differential operator with a non-singular kernel to cope with the fundamental theorem of fractional calculus. In addition to the prevailing non-integer order definitions, Khalil et al. [5] introduced a novel local-type fractional operator known as the conformable fractional derivative. It is a straightforward progression of the familiar limit definition of integer order derivative. Conformable calculus tends to the integer order calculus as its fractional order $\rho \to n \in \mathbb{N}$ for all of its terminologies, including conformable fractional differentiation and integration, conformable integral transforms, conformable integration by parts, conformable chain rule, conformable Green's theorem, conformable Stokes' theorem and conformable Gronwall's inequality [6, 7]. Furthermore, Atangana et al. [8] demonstrated its correlation with Riemann-Stieltjes integral and fractal derivatives, an established tool to study phenomenon associated with fractal dimensions and geometry [9, 10]. Thus, conformable derivative mergers fractional calculus with fractal geometry. Despite these advantageous features, it received several criticisms [11, 12]. Addressing the capabilities and challenges associated with existing definitions of fractional derivative is an active area of research. Potential future advancements may involve the establishment of more consistent and robust definitions of fractional derivative.

Shallow water waves or long waves are shallower than 1/20 of their actual wavelength. When waves travel into the region of shallow water, these are frequently influenced by the ocean floor. This disrupts the free water in orbital motion, rendering the water molecules incapable of returning to their initial position. In turn, this phenomenon causes environmental hazards, such as tsunami waves and coastal erosion. The dispersion regulates the intensity of a water wave. This dispersive behavior emerges either by interplay between waves, geometric configurations or physical constraints. Sailors employ shallow water wave models in simulations to enhance the realism of virtual maritime scenarios and generate reliable inputs for ship navigation systems. Therefore, dispersive shallow water wave models are of particular interest due to their significant legacy as instructors in the fields of tsunami forecasting, river flooding, ocean wave dynamics, coastal engineering and dam break problems [13-15].

In 1834, Russell's "Report on Waves" initiated a debate among the researchers on accounting, a challenge to the antecedent knowledge of waves [16]. Russell reported the feasibility of permanent profiles in shallow water as well, not only in deep water. Russell referred to this permanent profile as Wave of Translation. In 1895, using the primary equation of hydrodynamics, Korteweg and de Vries formulated a model entitled the Korteweg-de Vries (KdV) equation. The KdV equation is usually written as [17]:

$$\vartheta_t^{(\rho)} + \vartheta\vartheta_x + \vartheta_{xxx} = 0 \tag{1}$$

where α and β are constants. t and x are normalized temporal and spatial variables. Subscripts represent partial derivatives. The first term is an evolution term. The non-linearity is apparent from the second term; and the third term directs to the inclusion of third-order dispersion. This equation turns out to be key in explaining the primary idea of counterbalancing non-linear advection by the dispersion effect, which is responsible for the soliton phenomenon. In 1965, Zabusky and Krushal elaborated on the interaction phenomenon of solitons through a computational study of the KdV equation [18]. Solitons are found to be capable of reattaining their amplitudes, shape and an additional phase shift after the interaction. Initially, the KdV equation is formulated to describe the asymptotic dynamics of the lossless profile of long waves in shallow water. As time progresses, numerous scientific domains have benefited from the massive utilization of such a powerful equation. The KdV equation is used to replicate ion-acoustic waves [19], cosmic inflations [20], pressure gauges for liquid gas mixtures [21], wave generation in rotating fluids confined in tubes [22], tectonic dynamics and earthquake predictions [23]. Moreover, the enormous destructive ocean waves known as tsunamis that propagate from the epicenter of the undersea earthquake to the coastline are also precisely simulated by the KdV-type systems [13, 14]. Due to the enormous breadth of applications, several studies attempt the exposure of various wave conductance for equations from KdV hierarchy [24-32]. Multi-component KdV system explores the dynamics of co-existence and interaction phenomenon of multiple shallow water and long internal waves with different dispersion relations in multi-layered or density-stratified medium [24, 33]. The time fractional non-linear multi-component KdV system with third-order dispersion can be written as:

i. One component form:

$$\vartheta_t^{(\rho)} + \vartheta\vartheta_x + \vartheta_{xxx} = 0. \tag{2}$$

ii. Two component form:

$$\begin{aligned} &\phi_t^{(\rho)} + 6\alpha\phi\phi_x - 2\mu\psi\psi_x + \alpha\phi_{xxx} = 0, \\ &\psi_t^{(\rho)} + 3\beta\phi\psi_x + \beta\psi_{xxx} = 0. \end{aligned} \tag{3}$$

iii. Three component form:

$$\begin{aligned} &\phi_t^{(\rho)} = \frac{1}{4}\phi_{xxx} + 3\phi\phi_x - 6\psi\psi_x + 3\theta_x, \\ &\psi_t^{(\rho)} = -\frac{1}{2}\psi_{xxx} - 3\phi\psi_x, \\ &\theta_t = -\frac{1}{2}\theta_{xxx} - 3\phi\theta_x, \end{aligned} \tag{4}$$

where $\rho \in (0,1]$ is fractional order and corresponds to the definition of conformable derivative; α, β and μ are constants. Successive removal of wave functions in Eq. (4) as $\theta(x,t) = 0$ and $\psi(x,t) = 0$ reduces it to the preceding two component and one component forms, respectively. Figure 1 represents schematic configuration of the two component form of the KdV system in a two-layer water medium. η represents the elevation of interfaces and surfaces from equilibrium. The fractal-fractional conformable derivative order ρ accounts for non-uniform temporal evolution due to complex inter-layer wave interactions and density stratification effects.

Integral transforms are vibrant tools for mathematicians and scientists for the simplification that they serve in solving differential and integral equations. An appropriate selection of integral transform reduces partial differential equations (PDEs) to another PDE with one fewer independent variable; ordinary differential equations (ODEs) and integral equations are transformed into algebraic equations that are easier to solve. However, making the decision for a particular choice of an integral transform prior to its implementation is still based on ambiguous criteria. Jafari [34] showed how variation in only the coefficients of differential equations affects the efficacy of the integral transform in solving them. Therefore, if one integral transform is capable of handling a problem, the same level of efficiency cannot be assumed for other integral transforms. Each transform has its own theoretical and practical significance. Once again, integral transforms enticed the engagement of scientists and researchers because of their potential to solve fractional-order equations. Recently, in the subject of integral transforms, various notable transforms have been reported, such as Elzaki [35], Mohand [36], Aboodh [37], Natural [38], Sawi [39], Shehu [40], Yang [41], ARA [42], Formable [43], Kharrat-Toma [44] and J transforms [45]. In 2023, Arora and Pasrija [46] introduced a new integral transform called the generalized bivariate (GB) transform with a range class of applications than existing Laplace-like transforms. To date, all integral transforms have suffered from the limited applicability to non-linear equations. In the present study, motivated with the goal of broadening the application of the GB-transform to time-fractional non-linear equations, it is combined with homotopy perturbation method (HPM) to overcome the challenges of non-linearity [47].

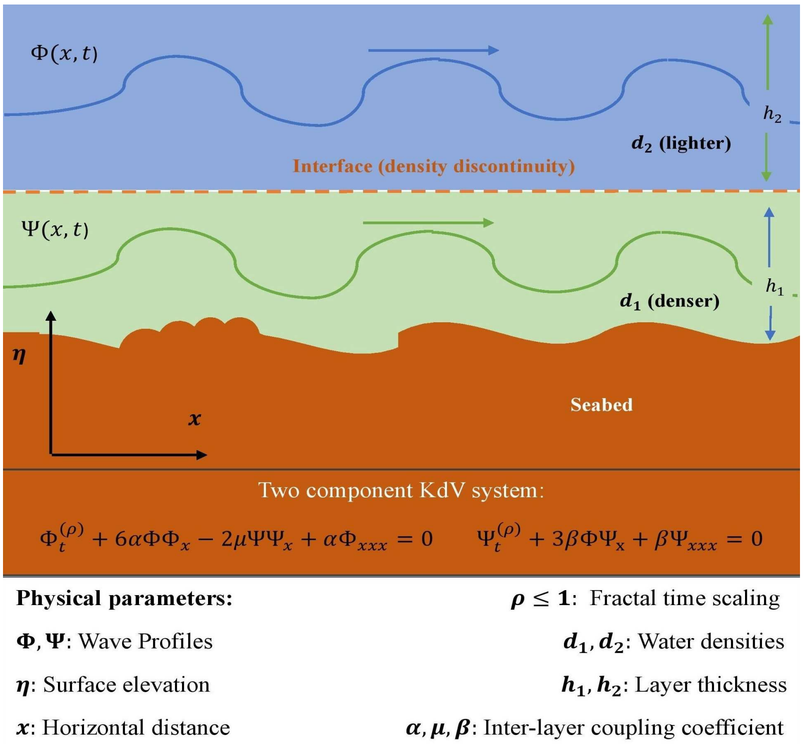

Fig. 1. Schematic configuration of the coupled KdV system in a two-layerwater medium.

HPM [48, 49] is formulated based on the concepts of homotopy and perturbation methods. This semi-analytic approach provides an explicit approximate solution in form of a truncated series expansion. The occasionally obtained closed-form of expansion solution represents the analytic solution. Unlike many conventional computational processes, HPM operates independently of assumption about small perturbation parameter, linearization procedure and the handling of ill-conditioned matrices. This versatile approach has been considered to solve PDEs, ODEs, integral and integro-differential equations [48-51].

The study is structured as follows: Section 2 presents the preliminaries of conformable calculus and the GB-transform. Section 3 elaborates on the methodology of the proposed generalized bivariate homotopy perturbation method (GB-HPM) scheme for time-fractional non-linear partial differential equations. Section 4 provides a theoretical analysis of the proposed scheme's convergence. Section 5 demonstrates the performance of the proposed scheme to capture the internal dynamics of fractional multi-component KdV system. Concluding remarks are presented at the end.

2. Preliminaries of Conformable Calculus and the GB-transform

Definition 1. Let $\vartheta(t):[0,\infty)\to\mathbb{R}$. Then, the fractional operator of order $\rho\in(0,1]$ in conformable sense is stated as [5]:

$$\vartheta_t^{(\rho)}(t) = \lim_{\delta\to 0}\frac{\vartheta(t+\delta t^{1-\rho})-\vartheta(t)}{\delta} \tag{5}$$

If $\vartheta(t)$ is $\rho-$differentiable in some $(0,c)$ where $c>0$ and the $\lim_{t\to 0^+}\vartheta_t^{(\rho)}(t)$ exists, then:

$$\vartheta_t^{(\rho)}(0) = \lim_{t\to 0^+}\vartheta_t^{(\rho)}(t). \tag{6}$$

Theorem 2. [5, 6] Let $0<\rho<1$ and $\vartheta=\vartheta(t)$, $\varsigma=\varsigma(t)$ be $\rho-$differentiable at $t>0$. Then:

(1) $(c_1\vartheta + c_2\varsigma)_t^{(\rho)} = c_1\vartheta_t^{(\rho)} + c_2\varsigma_t^{(\rho)}$.

(2) $(t^{\delta})_t^{(\rho)} = \delta t^{\delta-\rho}, \forall\delta\in\mathbb{R}$.

(3) $(\vartheta.\varsigma)_t^{(\rho)} = \vartheta\varsigma_t^{(\rho)} + \varsigma\vartheta_t^{(\rho)}$.

(4) $\left(\dfrac{\vartheta}{\varsigma}\right)_t^{(\rho)} = \dfrac{\varsigma\vartheta_t^{(\rho)} - \vartheta\varsigma_t^{(\rho)}}{\varsigma^2}$.

(5) $(\varphi)_t^{(\rho)} = 0, \varphi$ is constant.

Lemma 3. [6] If ϑ is differentiable, then:

$$\vartheta_t^{(\rho)} = t^{1-\rho}\frac{\partial\vartheta}{\partial t}. \tag{7}$$

Lemma 4. [5,6] Let $\vartheta:[a,b)\to\mathbb{R}$ be differentiable and $0<\rho\le 1$. Then for all $t>a$ fractional integral operator can be defined as:

$$I_a^{\rho}(\vartheta_t^{(\rho)})=\vartheta(t)-\vartheta(0). \tag{8}$$

Definition 5. [46] The integral operator, the GB-transform of δ order for the given function $\vartheta(t)$ is defined as:

$$\mathbb{A}_{\delta}[\vartheta(t)]=\mathbb{P}_{\delta}(\mu,\nu)=\frac{\mu}{\nu^{\delta}}\int_0^{\infty}t^{\delta-1}\exp\left(-\frac{\mu}{\nu}t\right)\vartheta(t)dt;\mu,\nu>0. \tag{9}$$

Definition 6. [46] The inverse operator of the GB-transform of $\delta-$ order is given by:

$$\mathbb{A}_{\delta}^{-1}[\mathbb{P}_{\delta}(\mu,\nu)]=\left(\frac{(-1)^{2(\delta-1)}}{2\pi i}\right)\int_{c-i\infty}^{c+i\infty}\left(\frac{1}{\nu}\right)\exp\left(\frac{\mu}{\nu}t\right)\mathbb{S}(\mu,\nu)ds, \tag{10}$$

where $\mathbb{S}(\mu,\nu)$ is Shehu transform of $\vartheta(t)$.

Theorem 7. [46] The GB-transform of $\vartheta_t^{(m)}(t)$ is given by:

$$\mathbb{A}_{\delta}[\vartheta^{(m)}(t)]=(-1)^{\delta-1}\left(\frac{\mu}{\nu}\right)\frac{\partial^{\delta-1}}{\partial\mu^{\delta-1}}\left[\left(\frac{\mu}{\nu}\right)^{m-1}\mathbb{A}_1[\vartheta(t)]=\sum_{k=0}^{m-1}\left(\frac{\mu}{\nu}\right)^{m-(k+1)}\vartheta^{(k)}(0)\right]. \tag{11}$$

3. General Procedure

To demonstrate the algorithm of the proposed methodology, consider a general partial differential equation with an arbitrary temporal order defined in conformable sense as:

$$\vartheta_t^{(\rho)}(x,t)=\Lambda[\vartheta(x,t)]+\Omega[\vartheta(x,t)]+s(x,t) \tag{12}$$

with initial condition:

$$\vartheta(x,0)=\varphi(x), \tag{13}$$

where Λ and Ω are linear and non-linear operators, respectively and $s(x,t)$ is the source term. $\rho\in(0,1]$ represents the non-integer order in conformable sense.

Applying the GB-transform of order ρ to Eq. (12) implies:

$$\frac{1}{\nu^{\rho-1}}\mathbb{A}_1\left[\frac{\partial\vartheta}{\partial t}\right]=\mathbb{A}_{\rho}[s(x,t)]+\mathbb{A}_{\rho}[\Lambda[\vartheta(x,t)]+\Omega[\vartheta(x,t)]]. \tag{14}$$

Using the application criteria of the GB-transform for differentiation with the given initial condition yields:

$$\mathbb{P}_1(x,\mu,\nu)=\varphi(x)+\frac{\nu^{\rho}}{\mu}\mathbb{A}_{\rho}[s(x,t)]+\frac{\nu^{\rho}}{\mu}\mathbb{A}_{\rho}[\Lambda[\vartheta(x,t)]+\Omega[\vartheta(x,t)]], \tag{15}$$

where $\mathbb{A}_1[\vartheta(x,t)]=\mathbb{P}_1(x,\mu,\nu)$.

Applying $\mathbb{A}_1^{-1}$ on both sides, gives:

$$\vartheta(x,t)=\varphi(x,t)+\mathbb{A}_1^{-1}\left[\frac{\nu^{\rho}}{\mu}\mathbb{A}_{\rho}[s(x,t)]\right]+\mathbb{A}_1^{-1}\left[\frac{\nu^{\rho}}{\mu}\mathbb{A}_{\rho}[\Lambda[\vartheta(x,t)]+\Omega[\vartheta(x,t)]]\right]. \tag{16}$$

At this step, to utilize the excellence of HPM, embed the homotopy parameter $h\in[0,1]$ in Eq. (16) as:

$$\vartheta(x,t)=G(x,t)+h\mathbb{A}_1^{-1}\left[\frac{\nu^{\rho}}{\mu}\mathbb{A}_{\rho}[\Lambda[\vartheta(x,t)]+\Omega[\vartheta(x,t)]]\right]. \tag{17}$$

where $G(x,t)$ arises from the source term and initial condition.

Let the solution $\vartheta(x,t)$ has infinite series expansion of the form:

$$\vartheta(x,t)=\sum_{j=0}^{\infty}h^j\vartheta_j(x,t). \tag{18}$$

The decomposition of non-linear term can be proposed as:

$$\Omega[\vartheta(x,t)]=\sum_{j=0}^{\infty}h^j\mathcal{P}_j, \tag{19}$$

where He's polynomials, $\mathcal{P}_k$ are stated as:

$$\mathcal{P}_k(\vartheta_0,\vartheta_1,\dots,\vartheta_k)=\frac{1}{k!}\frac{\partial^k}{\partial h^k}\left[\Omega\left(\sum_{j=0}^{\infty}h^j\vartheta_j(x,t)\right)\right]_{h=0}. \tag{20}$$

Inserting Eq. (18) and Eq. (19) in Eq. (17), gives:

$$\sum_{j}^{\infty} h^j \vartheta_j(x,t) = G(x,t) + h\mathbb{A}_1^{-1}\left[\frac{\nu^\rho}{\mu}\mathbb{A}_\rho\left[\Lambda\left[\sum_{j=0}^{\infty} h^j\vartheta_j(x,t)\right] + \Omega\left[\sum_{j=0}^{\infty} h^j\vartheta_j(x,t)\right]\right]\right]. \tag{21}$$

This represents the pairing of the GB-transform and HPM, enhanced by He's polynomials [52]. Thus, comparison of the coefficients of like powers of h yields:

$$\begin{aligned} &\vartheta_0(x,t) = G(x,t), \\ &\vartheta_1(x,t) = \mathbb{A}_1^{-1}\left[\frac{\nu^\rho}{\mu}\mathbb{A}_\rho[\Lambda[\vartheta_0(x,t)] + \mathcal{P}_0]\right]. \end{aligned} \tag{22}$$

In the same way, the general recurrence relation can be deduced as:

$$\vartheta_{m+1}(x,t) = \mathbb{A}_1^{-1}\left[\frac{\nu^\rho}{\mu}\mathbb{A}_\rho\left[\Lambda[\vartheta_m(x,t)] + \mathcal{P}_m\right]\right]. \tag{23}$$

This leads to the desired components of series solution given in Eq. (18) with $h = 1$.

4. Analysis of the GB-HPM Scheme

The time fractional KdV can be written as:

$$\vartheta_t^{(\rho)} = -\alpha\vartheta\vartheta_x - \beta\vartheta_{xxx}. \tag{24}$$

Let,

$$N(x,t,\vartheta,\alpha,\beta) = -\alpha\vartheta\vartheta_x - \beta\vartheta_{xxx}. \tag{25}$$

Lemma 8. The function N satisfies the Lipschitz condition.

Proof. Let ϑ and ϑ^* be two bounded functions. Using definition of N and triangular inequality gives:

$$\begin{aligned} &\|N(x,t,\vartheta,\alpha,\beta) - N(x,t,\vartheta^*,\alpha,\beta)\| \le |\alpha|\,\|\vartheta\vartheta_x - \vartheta^*\vartheta_x^*\| + |\beta|\,\|\vartheta_{xxx} - \vartheta_{xxx}^*\|, \\ &= \frac{1}{2}|\alpha|\,\|(\vartheta^2 - \vartheta^{*2})_x\| + |\beta|\,\|(\vartheta - \vartheta^*)_{xxx}\|. \end{aligned}$$

Now suppose that $\exists$ constants $\kappa_1, \kappa_2 > 0$ such that $\forall (x,t) \|\vartheta\| \le \kappa_1$ and $\|\vartheta^*\| \le \kappa_2$, $\kappa = \max\{\kappa_1, \kappa_2\}$. Then their first derivative fulfills Lipschitz condition and $\exists$ a non-negative number L_1 such that:

$$\begin{aligned} &\|N(x,t,\vartheta,\alpha,\beta) - N(x,t,\vartheta^*,\alpha,\beta)\| \le \frac{|\alpha|}{2}L_1\|\vartheta^2 - \vartheta^{*2}\| + |\beta|L_1^3\|\vartheta - \vartheta^*\|, \\ &\le \left(\frac{|\alpha|}{2}L_1\kappa + |\beta|L_1^3\right)\|\vartheta - \vartheta^*\|, \end{aligned} \tag{26}$$

where $\|\vartheta^2 - \vartheta^{*2}\| \le 2\kappa\|\vartheta - \vartheta^*\|$. Hence,

$$\|N(x,t,\vartheta,\alpha,\beta) - N(x,t,\vartheta^*,\alpha,\beta)\| \le L\|\vartheta - \vartheta^*\|,$$

where,

$$L = \left(\frac{|\alpha|}{2}L_1\kappa + |\beta|L_1^3\right).$$

The same process can be followed for estimation of Lipschitz constant for fractional two and three component form of KdV system.

Theorem 9. Let us assume that $\vartheta(x,t)$ and $\vartheta_j(x,t)$ be defined in complete normed linear space $\aleph$ with norm $\|\vartheta\| \le \max_{(x,t)\in J}|\vartheta(x,t)|$ on an interval *J*. Further, suppose linear and non-linear operators described in Section 3 are contraction operators with Lipschitz constants ω_1 and ω_2, respectively. Then, the GB-HPM solution converges when $0 < (\omega_1 + \omega_2)t^\rho / \rho < 1$.

Proof. Let $Y_m = \sum_{j=0}^{m}\vartheta_j(x,t)$. To show that sequence of partial sums Y_m is a Cauchy sequence in $\aleph$, consider:

$$\|Y_m - Y_n\| = \max_{(x,t)\in J}|Y_m - Y_n|,$$

$$= \max_{(x,t)\in J}\left|\sum_{j=n+1}^{m}\vartheta_j\right|,$$

$$\le \max_{(x,t)\in J}\left|\mathbb{A}_1^{-1}\frac{\nu^\rho}{\mu}\mathbb{A}_\rho\left[\sum_{j=n+1}^{m}(\Lambda[\vartheta_{j-1}] + \Omega[\vartheta_{j-1}])\right]\right|,$$

$$= \max_{(x,t)\in J}\left|\mathbb{A}_1^{-1}\frac{\nu^\rho}{\mu}\mathbb{A}_\rho\left[\sum_{j=n}^{m-1}(\Lambda[\vartheta_j]+\Omega[\vartheta_j])\right]\right|,$$

$$\le \max_{(x,t)\in J}\left|\mathbb{A}_1^{-1}\frac{\nu^\rho}{\mu}\mathbb{A}_\rho\left[\Lambda[\vartheta_{m-1}]-\Lambda[\vartheta_{n-1}]\right]\right| + \max_{(x,t)\in J}\left|\mathbb{A}_1^{-1}\frac{\nu^\rho}{\mu}\mathbb{A}_\rho\left[\Omega[\vartheta_{m-1}]-\Omega[\vartheta_{n-1}]\right]\right|,$$

$$\le (\omega_1+\omega_2)\frac{t^\rho}{\rho}\|\vartheta_{m-1}-\vartheta_{n-1}\|.$$

Let $m=n+1$, then:

$$\|\vartheta_{n+1}-\vartheta_{n-1}\| \le \omega\|\vartheta_n-\vartheta_{n-1}\| \le \omega^2\|\vartheta_{n-1}-\vartheta_{n-2}\| \le \ldots \le \omega^n\|\vartheta_1-\vartheta_0\|,$$

where $\omega=(\omega_1+\omega_2)t^\rho/\rho$. Similarly, one can deduce:

$$\|\vartheta_{m-1}-\vartheta_{n-1}\| \le \|\vartheta_{n+1}-\vartheta_n\| + \|\vartheta_{n+2}-\vartheta_{n+1}\| + \ldots + \|\vartheta_m-\vartheta_{m-1}\|,$$

$$\le (\omega^n+\omega^{n+1}+\ldots+\omega^{m-1})\|\vartheta_1-\vartheta_0\|,$$

$$\le \omega^n\left(\frac{1-\omega^{m-n}}{1-\omega}\right)\|\vartheta_0\|.$$

As $0<\omega<1$, this implies $1-\omega^{m-n}<1$. Therefore,

$$\|\mathrm{Y}_m-\mathrm{Y}_n\| \le \frac{\omega^n}{1-\omega}\|\vartheta_0\|. \tag{27}$$

Since $\|\vartheta_0\|<\infty$, as a result when $n\to\infty$ we get $\|\mathrm{Y}_m-\mathrm{Y}_n\|\to 0$. Hence, Y_m is a Cauchy sequence in $\aleph$. This fulfills the condition of convergence of the series solution.

Moreover, Eq. (27) implies error estimation of two approximate solutions for finite values of m and n. The case, $m\to\infty$ provides the error estimation between analytic and approximate solutions.

5. Numerical Performance

In this part, the series solution is obtained for the non-linear multi-component KdV system in framework of conformable time-fractional derivative.

Example 1. Consider Eq. (2) for $\alpha=6$ and $\beta=1$ as:

$$\vartheta_t^{(\rho)} + 6\vartheta\vartheta_x + \vartheta_{xxx} = 0. \tag{28}$$

subjected to the initial condition:

$$\vartheta(x,0) = \mathrm{sech}(x-1) + \mathrm{sech}(c-5) \tag{29}$$

Selecting linear operator, $\Lambda[\vartheta]=-\vartheta_{xxx}$, the non-linear operator, $\Omega[\vartheta]=-6\vartheta\vartheta_x$ and the source term, $s(x,t)=0$, Eq. (13) takes the form:

$$\frac{1}{\nu^{\rho-1}}\mathbb{A}_1\left[\frac{\partial\vartheta}{\vartheta t}\right] = \mathbb{A}_\rho[s(x,t)] + \mathbb{A}_\rho[-\vartheta_{xxx}-6\vartheta\vartheta_x]. \tag{30}$$

Using Theorem 7 with the given initial condition in Eq. (29) and re-arrangement of terms provides:

$$\mathbb{P}_1(x,\mu,\nu) = \varphi(x) + \frac{\nu^\rho}{\mu}\mathbb{A}_\rho[s(x,t)] + \frac{\nu^\rho}{\mu}\mathbb{A}_\rho[-\vartheta_{xxx}-6\vartheta\vartheta_x], \tag{31}$$

where $\mathbb{A}_1[\vartheta(x,t)]=\mathbb{P}_1(x,\mu,\nu)$. Employing the inverse GB-transform of order one, $\mathbb{A}_1^{-1}$ on both sides, yields:

$$\vartheta(x,t) = \varphi(x) + \mathbb{A}_1^{-1}\left[\frac{\nu^\rho}{\mu}\mathbb{A}_\rho[s(x,t)]\right] + \mathbb{A}_1^{-1}\left[\frac{\nu^\rho}{\mu}\mathbb{A}_\rho[-\vartheta_{xxx}-6\vartheta\vartheta_{xxx}]\right]. \tag{32}$$

Now, application of HPM associated with He's polynomials leads to:

$$\begin{aligned}
&\vartheta_0(x,t) = \mathrm{sech}(x-1) + \mathrm{sech}(x-5),\\
&\vartheta_{m+1}(x,t) = -\mathbb{A}_1^{-1}\left[\frac{\nu^\rho}{\mu}\mathbb{A}_\rho[(\vartheta_m)_{xxx}+6\mathcal{P}_m]\right]; m\ge 0,
\end{aligned} \tag{33}$$

where,

$$\begin{aligned}
&\mathcal{P}_0 = \vartheta_0(\vartheta_0)_x,\\
&\mathcal{P}_1 = \vartheta_0(\vartheta_1)_x + \vartheta_1(\vartheta_0)_x,\\
&\mathcal{P}_2 = \vartheta_0(\vartheta_2)_x + \vartheta_1(\vartheta_1)_x + \vartheta_2(\vartheta_0)_x,
\end{aligned} \tag{34}$$

Table 1. Absolute error in consecutive approximate solutions of Example 1.

		$\rho = 0.75$			$\rho = 1$		
x	t	$\lvert s\vartheta_2 - s\vartheta_1 \rvert$	$\lvert s\vartheta_3 - s\vartheta_2 \rvert$	$\lvert s\vartheta_4 - s\vartheta_3 \rvert$	$\lvert s\vartheta_2 - s\vartheta_1 \rvert$	$\lvert s\vartheta_3 - s\vartheta_2 \rvert$	$\lvert s\vartheta_4 - s\vartheta_3 \rvert$
-6	0.001	5.8009×10^{-8}	2.5236×10^{-10}	2.0947×10^{-12}	1.0318×10^{-9}	5.9870×10^{-13}	6.6279×10^{-16}
	0.002	1.6407×10^{-7}	1.2005×10^{-9}	1.6758×10^{-11}	4.1274×10^{-9}	4.7896×10^{-12}	1.0605×10^{-14}
	0.003	3.0142×10^{-7}	2.9892×10^{-9}	5.6558×10^{-11}	9.2866×10^{-9}	1.6165×10^{-11}	5.3686×10^{-14}
-4	0.001	6.9813×10^{-7}	7.4670×10^{-9}	9.3418×10^{-11}	1.2418×10^{-8}	1.7714×10^{-11}	2.9558×10^{-14}
	0.002	1.9746×10^{-6}	3.5519×10^{-8}	7.4734×10^{-10}	4.9673×10^{-8}	1.4172×10^{-10}	4.7293×10^{-13}
	0.003	3.6276×10^{-6}	8.8444×10^{-8}	2.5223×10^{-9}	1.1176×10^{-7}	4.7829×10^{-10}	2.3942×10^{-12}
-2	0.001	1.6974×10^{-5}	1.4648×10^{-7}	9.6800×10^{-9}	3.0193×10^{-7}	3.4751×10^{-10}	3.0628×10^{-12}
	0.002	4.8010×10^{-5}	6.9678×10^{-7}	7.7440×10^{-8}	1.2077×10^{-6}	2.7800×10^{-9}	4.9005×10^{-11}
	0.003	8.8199×10^{-5}	1.7350×10^{-6}	2.6136×10^{-7}	2.7174×10^{-6}	9.3826×10^{-9}	2.4809×10^{-10}
2	0.001	5.6795×10^{-5}	7.0391×10^{-6}	3.0397×10^{-6}	1.0103×10^{-6}	1.6699×10^{-8}	9.6179×10^{-10}
	0.002	1.6064×10^{-4}	3.3484×10^{-5}	2.4318×10^{-5}	4.0410×10^{-6}	1.3359×10^{-7}	1.5389×10^{-8}
	0.003	2.9512×10^{-4}	8.3375×10^{-5}	8.2073×10^{-5}	9.0923×10^{-6}	4.5088×10^{-7}	7.7905×10^{-8}
4	0.001	5.6795×10^{-5}	7.0391×10^{-6}	3.0397×10^{-6}	1.0103×10^{-6}	1.6699×10^{-8}	9.6179×10^{-10}
	0.002	1.6064×10^{-4}	3.3484×10^{-5}	2.4318×10^{-5}	4.0410×10^{-6}	1.3359×10^{-7}	1.5389×10^{-8}
	0.003	2.9512×10^{-4}	8.3375×10^{-5}	8.2073×10^{-5}	9.0923×10^{-6}	4.5088×10^{-7}	7.7905×10^{-8}
6	0.001	1.3267×10^{-5}	5.5129×10^{-6}	2.3975×10^{-6}	2.3599×10^{-7}	1.3079×10^{-8}	7.5857×10^{-10}
	0.002	3.7524×10^{-5}	2.6224×10^{-5}	1.9180×10^{-5}	9.4395×10^{-7}	1.0463×10^{-7}	1.2137×10^{-8}
	0.003	6.8936×10^{-5}	6.5299×10^{-5}	6.4731×10^{-5}	2.1239×10^{-6}	3.5312×10^{-7}	6.1444×10^{-8}

and so on; in this way, the remaining components of the assumed series solution can be obtained with $h = 1$ as described in Eq. (18). Thus, using the sum of the first three components, the approximate solution is:

$$\vartheta(x,t) = \operatorname{sech}(x-1) + \operatorname{sech}(x-5) + \frac{t^{\rho}}{\rho}\left[\left(\frac{6}{\cosh(x-1)} + \frac{6}{\cosh(x-5)}\right)\left(\frac{\sinh(x-1)}{\cosh^2(x-1)} + \frac{\sinh(x-5)}{\cosh^2(x-5)}\right)\right.$$

$$\left. - \frac{5\sinh(x-5)}{\cosh^2(x-5)} - \frac{5\sinh(x-1)}{\cosh^2(x-1)} + \frac{6\sinh^3(x-1)}{\cosh^4(x-1)} + \frac{6\sinh^3(x-5)}{\cosh^4(x-5)}\right] + \frac{t^{2\rho}}{2\rho^2}\left[\left(\frac{\sinh(x-1)}{\cosh^2(x-1)} + \frac{\sinh(x-5)}{\cosh^2(x-5)}\right)\right.$$

$$\left(6\left(\frac{6}{\cosh(x-1)} - \frac{6}{\cosh(x-5)}\right)\left(\frac{\sinh(x-1)}{\cosh^2(x-1)} + \frac{\sinh(x-5)}{\cosh^2(x-5)}\right) - \frac{30\sinh(x-5)}{\cosh^2(x-5)} - \frac{30\sinh(x-1)}{\cosh^2(x-1)}\right.$$

$$\left.\left. + \frac{36\sinh^3(x-5)}{\cosh^4(x-5)} + \frac{36\sinh^3(x-1)}{\cosh^4(x-1)}\right) + \left(\frac{6}{\cosh(x-1)} + \frac{6}{\cosh(x-5)}\right)\left(\left(\frac{\sinh(x-1)}{\cosh^2(x-1)} + \frac{\sinh(x-5)}{\cosh^2(x-5)}\right) + \dots\right.\right]$$

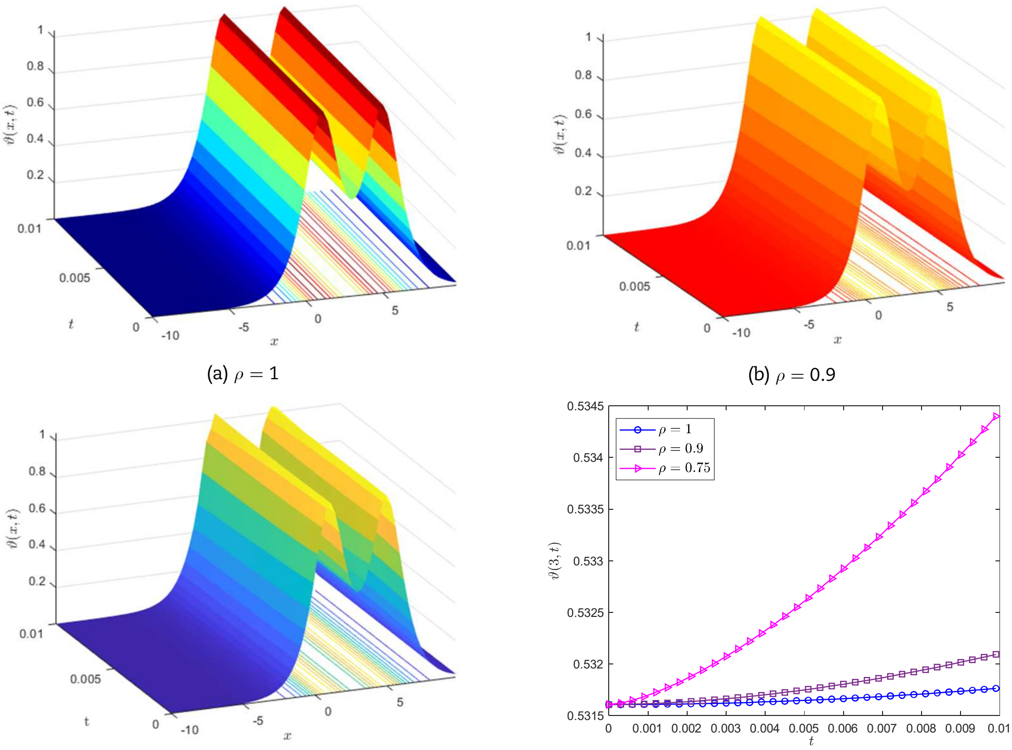

(a) $\rho = 1$ (b) $\rho = 0.9$ (c) $\rho = 0.75$ (d) $x = 3$

Fig. 2. Behavior of the approximate GB-HPM solution for Example 1.

The series solution to the investigated initial value problem anticipates the exploration of non-linear wave motion for given initial conditions. Figures 2(a,b,c) displays surface plots of the physical dynamics of non-linear wave propagation with varying fractional order $\rho = 1, 0.9, 0.75,$ respectively. Fig. 2(d) illustrates the deviation of the wave at $x = 3$ with a change in $\rho \to 1 \to 0.9 \to 0.75$ in the small interval of time. The considered initial condition led to the case of a symmetric profile about x = 3. Wave exhibits a local exicitement in spatial domain and swiftly tends to zero as $|x| \to \infty$.

Table 1 confirms the reliability of the results in terms of negligible absolute error between consecutive approximations $s\vartheta_m = \sum_{j=0}^{m} \vartheta_j(x,t)$. Hence, the hybridization of the GB-transform and HPM can be a breakthrough for fractional models that are still deprived of exact solutions. Moreover, the suggested integral transform is found to be a convenient tool to deal with conformable differentiation operator. It does not require any modification for the conformable differentiation operator, as the authors introduced it for Laplace, Sumudu, Natural, Elzaki and Mohand transforms to get rid of tedious calculation [53-57].

Example 2. Consider one component form given in Eq. (2) for initial data:

$$\vartheta(x,0) = \frac{12\gamma^2\beta}{\alpha}\operatorname{sech}^2(\gamma x), \tag{35}$$

for which exact solution takes the form as:

$$\partial(x,t) = \frac{12\gamma^2\beta}{\alpha}\operatorname{sech}^2(\gamma(x - 4\gamma^2\beta t)), \tag{36}$$

when $\rho = 1$ and α, β, γ are arbitrary constants. Applying the GB-HPM to Eq. (2) with choice of linear and non-linear operator as described in Example 1. This leads to the evaluation of undetermined components of series solution as following:

$$\begin{aligned}
\vartheta_1(x,t) &= \frac{96\beta^2\gamma^5 t^\rho \sinh(\gamma x)}{\alpha\rho\cosh^3(\gamma x)},\\
\vartheta_2(x,t) &= \frac{196\beta^3\gamma^8 t^{2\rho}(2\cosh^2(\gamma x) - 3)}{\alpha\rho^2\cosh^4(\gamma x)},\\
\vartheta_3(x,t) &= \frac{1024\beta^4\gamma^{11} t^{3\rho}\sinh(\gamma x)(\sinh^2(\gamma x) - 2)}{\alpha\rho^3\cosh^5(\gamma x)},\\
&\vdots
\end{aligned} \tag{37}$$

More components can be evaluated in the same manner. The truncated sum of series $s\vartheta_m = \sum_{j=0}^{m} \vartheta_j(x,t)$ will produce m^{th}-order approximate solution.

For $\gamma = 1/2, \alpha = 6$ and $\beta = 1$ the initial condition takes the form as $\vartheta(x,0) = [\operatorname{sech}^2(x/2)]/2$. This initial data initializes the dynamics of single soliton in the system as shown in Fig. 3. The wave $\vartheta(x,t)$ bifurcates into two waves as fractional order ρ decreases. On similar note the single bell-shaped soliton waveform is resulted with consideration of initial data $\vartheta(x,0) = 6\gamma^2\operatorname{sech}^2(\gamma x)$ for $\alpha = 1$ and $\beta = 1/2$. For initial data $\vartheta(x,0) = 6\operatorname{sech}^2(x)$ with $\gamma = 1, \alpha = 6$ and $\beta = 1$ solution interprets the propagation of two soliton phenomenon and its fractional dynamics, as shown in Fig. 4. Moreover, each subfigure emphasizes insight into the fractional dynamic nature of the system subject to the considered initial data. Small value of ρ displays the evolution of second soliton from its early stage. Table 2 and Table 3 provide a comparative assessment of the accuracy of derived results by GB-HPM against modified generalized Mittag-Leffler function method (MGMLFM) [58], residual power series method (RPSM) [59], reduced differential transform method (RDTM) [60] and modified fractional reduced differential transform method (MFRDTM) [61] in terms of absolute error. These tables showcase the supremacy of GB-HPM method. In Table 4 the calculated error of successive sums of series solution offers the view of convergence and reliability for fractional order $(\rho = 0.75)$ where exact solution is not available when $\rho < 1$.

Table 2. Comparative analysis of GB-HPM error with $\text{RPSM}_{5\text{th-order}}$ [59] and $\text{RDTM}_{4\text{th-order}}$ [60] errors for Example 2 when $\vartheta(x,0) = [\operatorname{sech}^2(x/2)]/2$ at $x = 10$.

t	$\text{GB-HPM}_{5\text{th-order}}$	[59]	$\text{GB-HPM}_{4\text{th-order}}$	[60]
0	0	0	0	0
0.1	1.2719×10^{-13}	1.8481×10^{-13}	7.6719×10^{-12}	7.6719×10^{-12}
0.2	8.2578×10^{-12}	1.0100×10^{-11}	2.4969×10^{-10}	2.4969×10^{-10}
0.3	9.5445×10^{-11}	1.0939×10^{-10}	1.9288×10^{-9}	1.9288×10^{-9}
0.4	5.4424×10^{-10}	6.0263×10^{-10}	8.2700×10^{-9}	8.2700×10^{-9}
0.5	2.1072×10^{-9}	2.2836×10^{-9}	2.5684×10^{-8}	2.5684×10^{-8}
0.6	6.3877×10^{-9}	6.8197×10^{-9}	6.5055×10^{-8}	6.5055×10^{-8}
0.7	1.6354×10^{-8}	1.7268×10^{-8}	1.4316×10^{-7}	1.4316×10^{-7}
0.8	3.7005×10^{-8}	3.8733×10^{-8}	2.8423×10^{-7}	2.8423×10^{-7}
0.9	7.6196×10^{-8}	7.9186×10^{-8}	5.2170×10^{-7}	5.2170×10^{-7}
1	1.4565×10^{-7}	1.5045×10^{-7}	9.0012×10^{-7}	9.0012×10^{-7}

Table 3. Comparative analysis of GB-HPM error with $\text{MGMLFM}_{3\text{rd-order}}$ [58] error for Example 2 when $\vartheta(x,0) = 6\gamma^2\operatorname{sech}^2(\gamma x)$ at $x = 30$.

γ	t	$s\vartheta_3$	Exact	$\text{GB-HPM}_{3\text{rd-order}}$	[58]
0.1	5	6.0386×10^{-4}	6.0386×10^{-4}	3.6707×10^{-12}	4.1582×10^{-9}
	15	6.2837×10^{-4}	6.2838×10^{-4}	2.9953×10^{-10}	3.9106×10^{-8}
	25	6.5388×10^{-4}	6.5388×10^{-4}	2.3283×10^{-9}	1.1254×10^{-7}
0.01	5	5.4909×10^{-4}	5.4909×10^{-4}	1.4073×10^{-19}	7.5835×10^{-14}
	15	5.4909×10^{-4}	5.4909×10^{-4}	1.7544×10^{-19}	6.8253×10^{-13}
	25	5.4910×10^{-4}	5.4910×10^{-4}	8.2679×10^{-20}	1.8959×10^{-12}
0.001	5	5.9946×10^{-6}	5.9946×10^{-6}	7.2631×10^{-22}	8.4703×10^{-22}
	15	5.9946×10^{-6}	5.9946×10^{-6}	1.7115×10^{-21}	4.2352×10^{-21}
	25	5.9946×10^{-6}	5.9946×10^{-6}	1.6133×10^{-21}	1.5247×10^{-20}

Table 4. Error analysis for Example 2 when $\vartheta(x,0)=6\,\mathrm{sech}^2(x)$.

		$\rho=0.75$			$\rho=1$		
x	t	$\lvert s\vartheta_2 - s\vartheta_1 \rvert$	$\lvert s\vartheta_3 - s\vartheta_2 \rvert$	$\lvert s\vartheta_4 - s\vartheta_3 \rvert$	$s\vartheta_2$	Exact	GB-HPM$_{\text{2nd-order}}$, [61]
-6	0.001	2.6566×10^{-7}	5.3693×10^{-9}	8.7499×10^{-11}	1.4628×10^{-4}	1.4628×10^{-4}	1.2710×10^{-11}
	0.002	7.5140×10^{-7}	2.5541×10^{-8}	6.9999×10^{-10}	1.4512×10^{-4}	1.4512×10^{-4}	1.0146×10^{-10}
	0.003	1.3804×10^{-6}	6.3597×10^{-8}	2.3625×10^{-9}	1.4396×10^{-4}	1.4396×10^{-4}	3.4170×10^{-10}
-4	0.001	1.5608×10^{-5}	4.8334×10^{-7}	2.7995×10^{-8}	7.9811×10^{-3}	7.9811×10^{-3}	1.1379×10^{-9}
	0.002	4.4147×10^{-5}	2.2992×10^{-6}	2.2396×10^{-7}	7.9171×10^{-3}	7.9171×10^{-3}	9.0348×10^{-9}
	0.003	8.1103×10^{-5}	5.7251×10^{-6}	7.5587×10^{-7}	7.8537×10^{-3}	7.8537×10^{-3}	3.0266×10^{-8}
-2	0.001	3.7233×10^{-3}	5.0865×10^{-4}	5.8351×10^{-5}	4.1932×10^{-1}	4.1931×10^{-1}	1.1885×10^{-6}
	0.002	1.0531×10^{-2}	2.4196×10^{-3}	4.6681×10^{-4}	4.1486×10^{-1}	4.1485×10^{-1}	9.3653×10^{-6}
	0.003	1.9347×10^{-2}	6.0248×10^{-3}	1.5755×10^{-3}	4.1054×10^{-1}	4.1050×10^{-1}	3.1138×10^{-5}
2	0.001	3.7233×10^{-3}	5.0865×10^{-4}	5.8351×10^{-5}	4.2863×10^{-1}	4.2863×10^{-1}	1.2254×10^{-6}
	0.002	1.0531×10^{-2}	2.4196×10^{-3}	4.6681×10^{-4}	4.3348×10^{-1}	4.3349×10^{-1}	9.9564×10^{-6}
	0.003	1.9347×10^{-2}	6.0248×10^{-3}	1.5755×10^{-3}	4.3847×10^{-1}	4.3850×10^{-1}	3.4133×10^{-5}
4	0.001	1.5608×10^{-5}	4.8334×10^{-7}	2.7995×10^{-8}	8.1108×10^{-3}	8.1108×10^{-3}	1.1556×10^{-9}
	0.002	4.4147×10^{-5}	2.2992×10^{-6}	2.2396×10^{-7}	8.1765×10^{-3}	8.1765×10^{-3}	9.3183×10^{-9}
	0.003	8.1103×10^{-5}	5.7251×10^{-6}	7.5587×10^{-7}	8.2427×10^{-3}	8.2428×10^{-3}	3.1702×10^{-8}
6	0.001	2.6566×10^{-7}	5.3693×10^{-9}	8.7499×10^{-11}	1.4864×10^{-4}	1.4864×10^{-4}	1.2766×10^{-11}
	0.002	7.5140×10^{-7}	2.5541×10^{-8}	6.9999×10^{-10}	1.4984×10^{-4}	1.4984×10^{-4}	1.0235×10^{-10}
	0.003	1.3804×10^{-6}	6.3597×10^{-8}	2.3625×10^{-9}	1.5104×10^{-4}	1.5104×10^{-4}	3.4619×10^{-10}

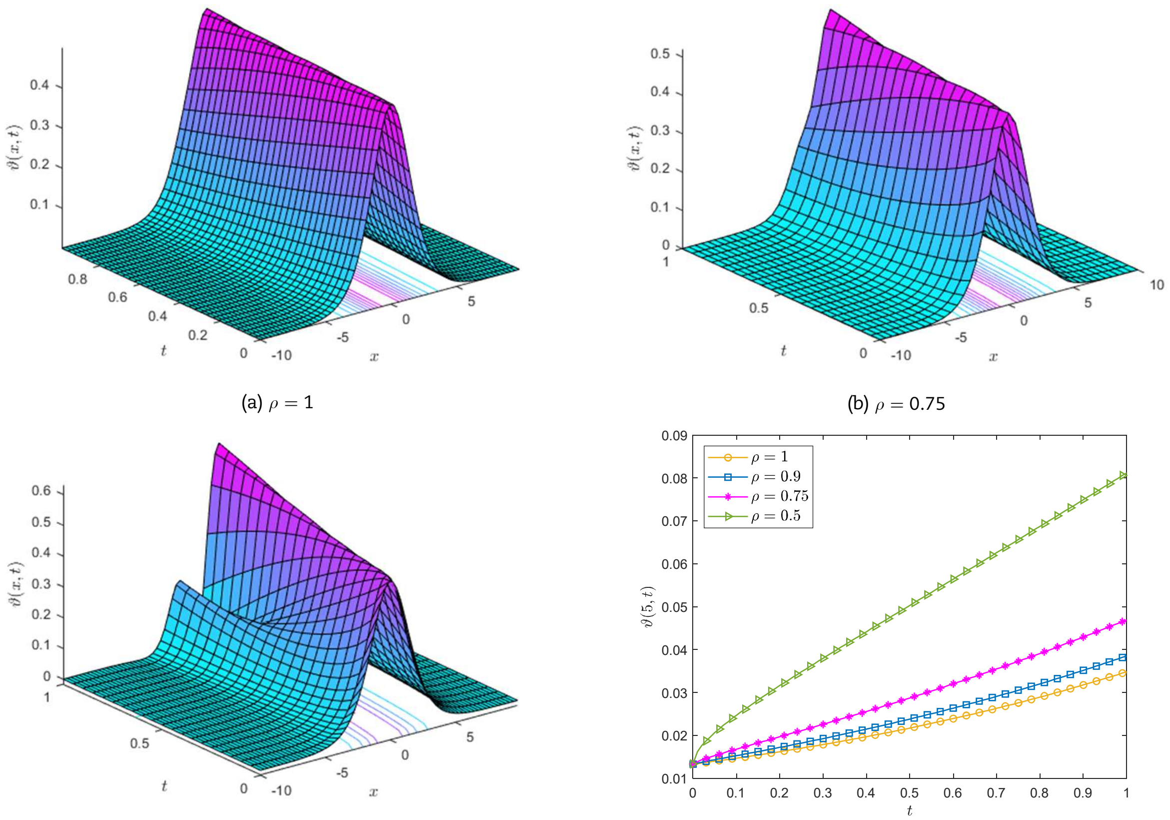

(a) $\rho=1$ (b) $\rho=0.75$ (c) $\rho=0.5$ (d) x = 5

Fig. 3. Behavior of the approximate GB-HPM solution for Example 2 when $\vartheta(x,0)=[\mathrm{sech}^2(x/2)]/2$.

Example 3. Consider two component forms of KdV system given in Eq. (3) for $\alpha=1$, $\mu=3/2$, $\beta=1$ as:

$$\begin{aligned} &\phi_t^{(\rho)} + 6\phi\phi_x - 3\psi\psi_x + \phi_{xxx} = 0, \\ &\psi_t^{(\rho)} + 3\phi\psi_x + \psi_{xxx} = 0, \end{aligned} \tag{38}$$

subject to the initial data:

$$\phi(x,0)=\psi(x,0)=\frac{4c^2e^{cx}}{(1+e^{cx})^2}. \tag{39}$$

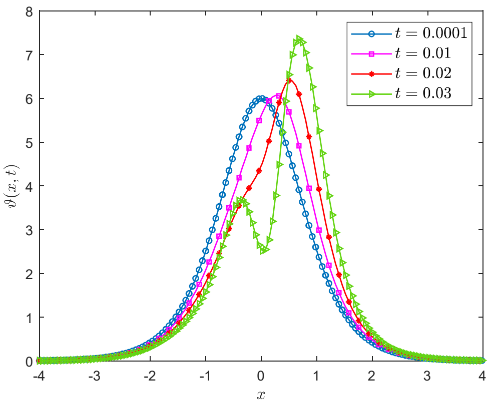

(a) $\rho = 1$

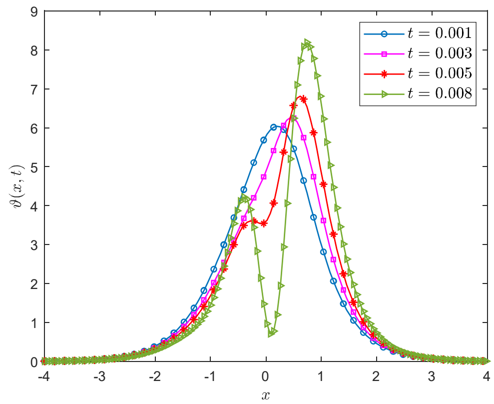

(b) $\rho = 0.75$

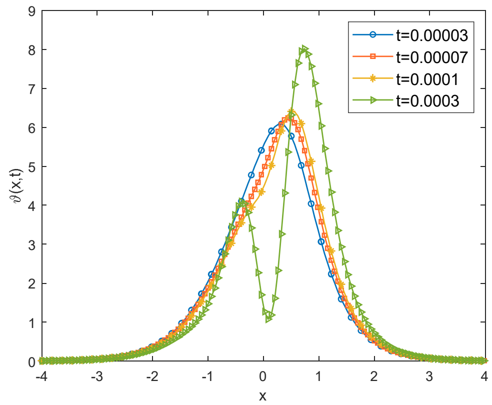

(c) $\rho = 0.5$

Fig. 4. Behavior of the approximate GB-HPM solution for Example 2 when $\vartheta(x,0) = 6\,\mathrm{sech}^2(x)$.

The exact solution specifically for $\rho = 1$ can be written as:

$$\phi(x,t) = \psi(x,t) = \frac{4c^2 e^{c(x-c^2t)}}{(1+e^{c(x-c^2t)})^2}. \tag{40}$$

where c is arbitrary constant. Applying $\mathbb{A}_\rho$ followed by $\mathbb{A}_1^{-1}$ and insertion of homotopy parameter yields:

$$\begin{aligned} \phi(x,t) &= \phi(x,0) + h\mathbb{A}_1^{-1}\left[\frac{\nu^\rho}{\mu}\mathbb{A}_\rho[-6\phi\phi_x + 3\psi\psi_x - \phi_{xxx}]\right], \\ \psi(x,t) &= \psi(x,0) + h\mathbb{A}_1^{-1}\left[\frac{\nu^\rho}{\mu}\mathbb{A}_\rho[-3\phi\psi_x - \psi_{xxx}]\right]. \end{aligned} \tag{41}$$

Implementing the expansion methodology, the solution can be considered as:

$$\begin{aligned} \phi(x,t) &= \sum_{j=0}^{\infty} h^j \phi_j(x,t), \\ \psi(x,t) &= \sum_{j=0}^{\infty} h^j \psi_j(x,t). \end{aligned} \tag{42}$$

Following the general procedure of GB-HPM the recursive relation for components of series solution can be obtained as:

$$\begin{aligned} \phi_0(x,t) &= \frac{4c^2 e^{cx}}{(1+e^{cx})^2}, \\ \psi_0(x,t) &= \frac{4c^2 e^{cx}}{(1+e^{cx})^2}, \\ \phi_{m+1}(x,t) &= \mathbb{A}_1^{-1}\left[\frac{\nu^\rho}{\mu}\mathbb{A}_\rho[-(\phi_m)_{xxx} + \mathcal{P}_m]\right], \\ \psi_{m+1}(x,t) &= \mathbb{A}_1^{-1}\left[\frac{\nu^\rho}{\mu}\mathbb{A}_\rho[-(\psi_m)_{xxx} + Q_m]\right], m \geq 0. \end{aligned} \tag{43}$$

where,

$$\begin{aligned}&\mathcal{P}_0=-6\phi_0(\phi_0)_x+3\psi_0(\psi_0)_x,\\&Q_0=-3\phi_0(\psi_0)_x,\\&\mathcal{P}_1=-6\phi_0(\phi_1)_x-6\phi_1(\phi_0)_x+3\psi_0(\psi_1)_x+3\psi_1(\psi_0)_x,\\&Q_1=-3\phi_0(\psi_1)_x-3\phi_1(\psi_0)_x,\\&\vdots\end{aligned}$$

For $h=1$, the components of the series solution can be deduced as:

$$\begin{aligned}\phi_1(x,t)&=\frac{4c^5t^{\rho}e^{cx}(e^{cx}-1)}{\rho(e^{cx}+1)^3},\\\psi_1(x,t)&=\frac{4c^5t^{\rho}e^{cx}(e^{cx}-1)}{\rho(e^{cx}+1)^3},\\\phi_2(x,t)&=\frac{2c^8t^{2\rho}e^{cx}(e^{2cx}-4e^{cx}+1)}{\rho^2(e^{cx}+1)^4},\\\psi_2(x,t)&=\frac{2c^8t^{2\rho}e^{cx}(e^{2cx}-4e^{cx}+1)}{\rho^2(e^{cx}+1)^4},\\&\vdots\end{aligned}\tag{44}$$

This procedure can be continued to calculate more components of the series solutions. Figure 5 represents the graphical visuals of the obtained 3^{rd}– order approximate series $s\phi_3$ and $s\psi_3$ of KdV system for $c=1$. These visuals indicate the approach of fractional profile to the exact solution with increment in fractional order ρ. The numerical results given in Table 5 simulate the agreement of GB-HPM results with prevailing natural decomposition method (NDM) [62] and generalized differential transform method (GDTM) [63] techniques. NDM combines natural transform with Adomain polynomials. The application of NDM is somewhat constrained due to the complex procedure to determine the Adomian polynomials [52]. Table 6 demonstrates the closeness of consecutive partial sums of series solutions for $\rho=0.75$. The decreasing absolute error assures the convergence and reliability of obtained results for fractional order $(\rho=0.75)$, when an exact solution is not available. Thus GB-HPM prevails over the restriction of an unknown exact solution to check the precision of obtained results.

Example 4. Consider three component forms of KdV system given in Eq. (4) for initial data that can be extracted from the exact solution:

$$\begin{aligned}\phi(x,t)&=\frac{p}{3k}-\frac{2k^2}{\left(kx-\frac{pt^{\rho}}{\rho}+\omega\right)^2},\\\psi(x,t)&=\frac{3c_2-4kp}{6k^2}+\frac{k^2}{\left(kx-\frac{pt^{\rho}}{\rho}+\omega\right)^2},\\\theta(x,t)&=c_0+\frac{c_2}{\left(kx-\frac{pt^{\rho}}{\rho}+\omega\right)^2},\end{aligned}\tag{45}$$

where p, k, ω, c_0 and c_2 are arbitrary constants.

Table 5. Error analysis of GB-HPM error with NDM [62] and GDTM [63] errors for Example 3.

x	t	$s\phi_2$	ϕ_{exact}	$\lvert s\phi_2-\phi_{exact}\rvert$ [62, 63]	$s\psi_2$	ψ_{exact}	$\lvert s\psi_2-\psi_{exact}\rvert$ [62, 63]
-10	0.1	5.1028×10^{-6}	4.0315×10^{-7}	2.3880×10^{-8}	5.1028×10^{-6}	4.0315×10^{-7}	2.3880×10^{-8}
	0.2	1.4433×10^{-5}	1.9177×10^{-6}	1.9104×10^{-7}	1.4433×10^{-5}	1.9177×10^{-6}	1.9104×10^{-7}
-5	0.1	7.1767×10^{-4}	5.3636×10^{-5}	2.8220×10^{-6}	7.1767×10^{-4}	5.3636×10^{-5}	2.8220×10^{-6}
	0.2	2.0299×10^{-3}	2.5514×10^{-4}	2.2576×10^{-5}	2.0299×10^{-3}	2.5514×10^{-4}	2.2576×10^{-5}
5	0.1	7.1767×10^{-4}	5.3636×10^{-5}	2.8222×10^{-6}	7.1767×10^{-4}	5.3636×10^{-5}	2.8222×10^{-6}
	0.2	2.0299×10^{-3}	2.5514×10^{-4}	2.2578×10^{-5}	2.0299×10^{-3}	2.5514×10^{-4}	2.2578×10^{-5}
10	0.1	5.1028×10^{-6}	4.0315×10^{-7}	2.3879×10^{-8}	5.1028×10^{-6}	4.0315×10^{-7}	2.3879×10^{-8}
	0.2	1.4433×10^{-5}	1.9177×10^{-6}	1.9103×10^{-7}	1.4433×10^{-5}	1.9177×10^{-6}	1.9104×10^{-7}

Table 6. Absolute error in consecutive approximate solutions of Example 3 for $\rho=0.75$.

x	t	$\lvert s\phi_2-s\phi_1\rvert$	$\lvert s\phi_3-s\phi_2\rvert$	$\lvert s\phi_4-s\phi_3\rvert$	$\lvert s\psi_2-s\psi_1\rvert$	$\lvert s\psi_3-s\psi_2\rvert$	$\lvert s\psi_4-s\psi_3\rvert$
-10	0.1	5.1028×10^{-6}	4.0315×10^{-7}	2.3880×10^{-8}	5.1028×10^{-6}	4.0315×10^{-7}	2.3880×10^{-8}
	0.2	1.4433×10^{-5}	1.9177×10^{-6}	1.9104×10^{-7}	1.4433×10^{-5}	1.9177×10^{-6}	1.9104×10^{-7}
-5	0.1	7.1767×10^{-4}	5.3636×10^{-5}	2.8220×10^{-6}	7.1767×10^{-4}	5.3636×10^{-5}	2.8220×10^{-6}
	0.2	2.0299×10^{-3}	2.5514×10^{-4}	2.2576×10^{-5}	2.0299×10^{-3}	2.5514×10^{-4}	2.2576×10^{-5}
5	0.1	7.1767×10^{-4}	5.3636×10^{-5}	2.8222×10^{-6}	7.1767×10^{-4}	5.3636×10^{-5}	2.8222×10^{-6}
	0.2	2.0299×10^{-3}	2.5514×10^{-4}	2.2578×10^{-5}	2.0299×10^{-3}	2.5514×10^{-4}	2.2578×10^{-5}
10	0.1	5.1028×10^{-6}	4.0315×10^{-7}	2.3879×10^{-8}	5.1028×10^{-6}	4.0315×10^{-7}	2.3879×10^{-8}
	0.2	1.4433×10^{-5}	1.9177×10^{-6}	1.9103×10^{-7}	1.4433×10^{-5}	1.9177×10^{-6}	1.9104×10^{-7}

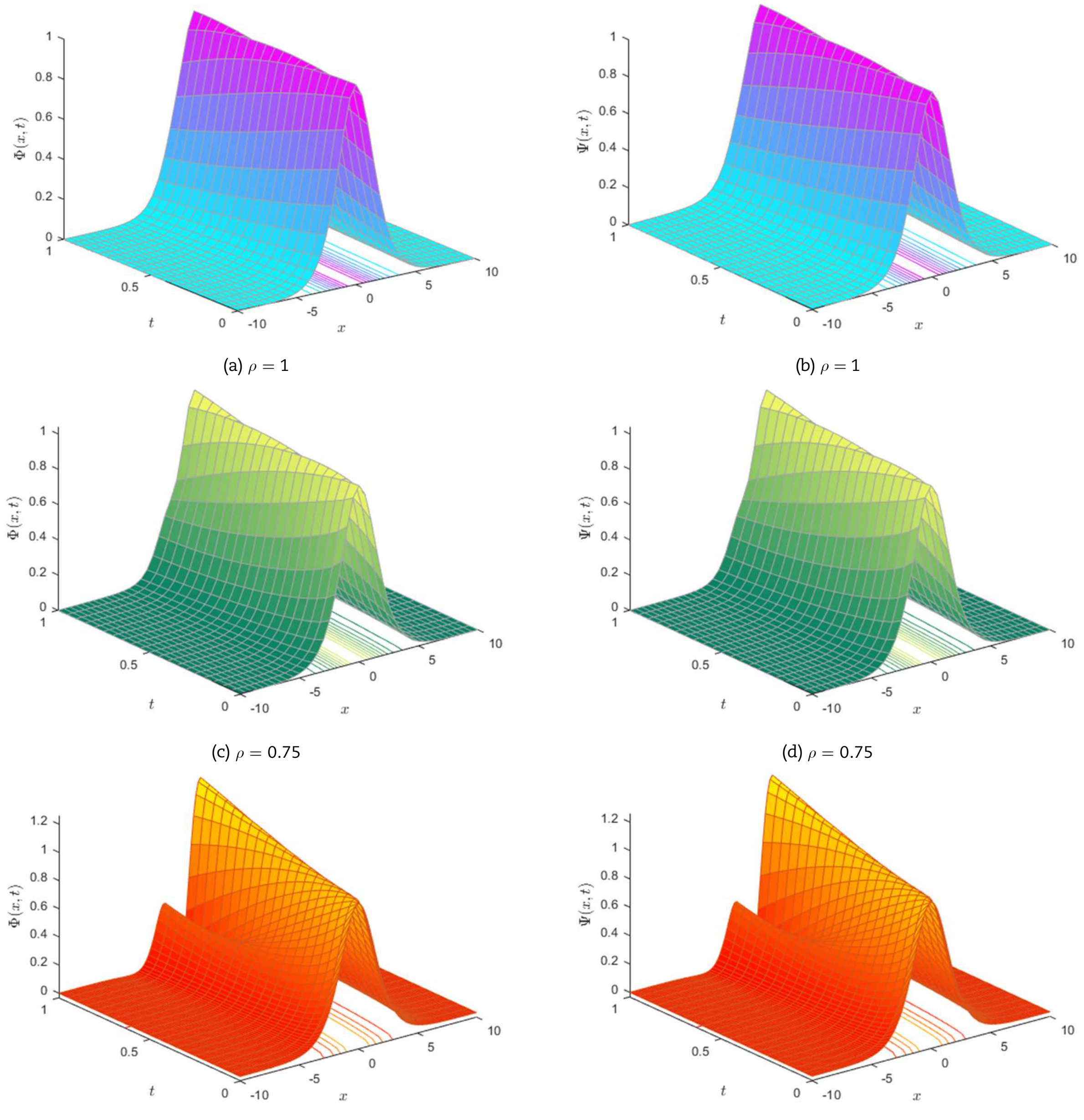

(a) $\rho = 1$ (b) $\rho = 1$

(c) $\rho = 0.75$ (d) $\rho = 0.75$

(e) $\rho = 0.5$ (f) $\rho = 0.5$

Fig. 5. Behavior of the approximate GB-HPM solution for Example 3 where (a, c, e) depict sϕ_3 and (b, d, f) depict sψ_3.

Applying $\mathbb{A}_\rho$ followed by $\mathbb{A}_1^{-1}$ and insertion of homotopy parameter yields:

$$\begin{aligned} \phi(x,t) &= \phi(x,0) + h\mathbb{A}_1^{-1}\left[\frac{\nu^\rho}{\mu}\mathbb{A}_\rho\left[\frac{1}{4}\phi_{xxxx} + 3\phi\phi_x - 6\psi\psi_x + 3\theta_x\right]\right], \\ \psi(x,t) &= \psi(x,0) + h\mathbb{A}_1^{-1}\left[\frac{\nu^\rho}{\mu}\mathbb{A}_\rho\left[-\frac{1}{2}\psi_{xxx} - 3\phi\psi_x\right]\right], \\ \theta(x,t) &= \theta(x,0) + h\mathbb{A}_1^{-1}\left[\frac{\nu^\rho}{\mu}\mathbb{A}_\rho\left[-\frac{1}{2}\theta_{xxx} - 3\phi\theta_x\right]\right]. \end{aligned} \tag{46}$$

Implementing the expansion methodology, the solution can be considered as:

$$\begin{aligned} \phi(x,t) &= \sum_{j=0}^{\infty} h^j\phi_j(x,t), \\ \psi(x,t) &= \sum_{j=0}^{\infty} h^j\psi_j(x,t), \\ \theta(x,t) &= \sum_{j=0}^{\infty} h^j\theta_j(x,t). \end{aligned} \tag{47}$$

Following the general procedure of GB-HPM the recursive relation for components of series solution can be obtained as:

$$\phi_0(x,t) = \frac{p}{3k} - \frac{2k^2}{(kx+\omega)^2},$$
$$\psi_0(x,t) = \frac{3c_2 - 4kp}{6k^2} + \frac{k^2}{(kx+\omega)^2},$$
$$\theta_0(x,t) = c_0 + \frac{c_2}{\left(kx - \frac{pt^\rho}{\rho} + \omega\right)^2},$$
$$\phi_{m+1}(x,t) = \mathbb{A}_1^{-1}\left[\frac{\nu^\rho}{\mu}\mathbb{A}_\rho\left[\frac{1}{4}(\phi_m)_{xxxx} + 3(\theta_m)_x + \mathcal{P}_m\right]\right],$$
$$\psi_{m+1}(x,t) = \mathbb{A}_1^{-1}\left[\frac{\nu^\rho}{\mu}\mathbb{A}_\rho\left[-\frac{1}{2}(\psi_m)_{xxx} + Q_m\right]\right],$$
$$\theta_{m+1}(x,t) = \mathbb{A}_1^{-1}\left[\frac{\nu^\rho}{\mu}\mathbb{A}_\rho\left[-\frac{1}{2}(\theta_m)_{xxx} + \mathcal{R}_m\right]\right], m \geq 0.$$

where,

$$\mathcal{P}_0 = 3\phi_0(\phi_0)_x - 6\psi_0(\psi_0)_x,$$
$$Q_0 = -3\phi_0(\psi_0)_x,$$
$$\mathcal{R}_0 = -3\phi_0(\theta_0)_x,$$
$$\mathcal{P}_1 = 3\phi_0(\phi_1)_x + 3\phi_1(\phi_0)_x - 6\psi_0(\psi_1)_x - 6\psi_1(\psi_0)_x,$$
$$Q_1 = -3\phi_0(\psi_1)_x - 3\phi_1(\psi_0)_x,$$
$$\mathcal{R}_1 = -3\phi_0(\theta_1)_x - 3\phi_1(\theta_0)_x,$$
$$\vdots$$

For $h = 1$, the components of the series solution given in Eq. (47) can be deduced as:

$$\begin{aligned} \phi_1(x,t) &= \frac{-(4k^2pt^\rho)}{\rho(\omega+kx)^3}, \\ \psi_1(x,t) &= \frac{2k^2pt^\rho}{\rho(\omega+kx)^3}, \\ \theta_1(x,t) &= \frac{2c_2pt^\rho}{\rho(\omega+kx)^3}, \\ \phi_2(x,t) &= \frac{-(6k^2p^2t^{2\rho})}{\rho^2(\omega+kx)^4}, \\ \psi_2(x,t) &= \frac{3k^2p^2t^{2\rho}}{\rho^2(\omega+kx)^4}, \\ \theta_2(x,t) &= \frac{3c_2p^2t^{2\rho}}{\rho^2(\omega+kx)^4}, \\ &\vdots \end{aligned} \tag{48}$$

Proceeding in the same manner leads to the determination of further components of the series solution. In Fig. 6, approximate $s\phi_3$, $s\psi_3$ and $s\theta_3$ are expressed for different fractional orders, i.e., $\rho = 0.25, 0.5, 0.75$. The quantity $\phi(x,t)$ represents the inner wave whereas $\psi(x,t)$ and $\theta(x,t)$ accounts for the surface waves. These visualizations aid in revealing the noticeable influence of fractional order on the amplitudes of the waves for $p = 0.5$, $k = 1$, $\omega = 1$ and $c_0 = c_2 = 1.5$. As a whole, the solution profiles appear to be stable; however, micro deviation can be observed at trough of and crust of $\psi(x,t)$ and $\theta(x,t)$ for smaller values of ρ. The derived GB-HPM results are closely aligned with exact and RPSM [15] results, as evident in Table 7. Errors are found to be of order between 10^{-6} and 10^{-10}. Error exhibits an inverse relationship with the fractional order ρ which also signifies the direct relation of convergence of GB-HPM solution with fractional order ρ. Comparing the methodology of GB-HPM to RPSM, suggested method does not require repeated evaluation of a function's fractional order derivative. This feature of GB-HPM enhances it to get over the limitations of RPSM to analyze the fractional phenomenon.

Table 7. Error analysis for Example 4 when $\omega = 1, p = 0.5, k = 1, c_0 = 1.5, c_2 = 1.5$ and $x = 10$.

	$\rho = 0.5$			$\rho = 0.75$		
t	$\lvert s\phi_3 - \phi_{exact}\rvert$	$\lvert s\psi_3 - \psi_{exact}\rvert$	$\lvert s\theta_3 - \theta_{exact}\rvert$	$\lvert s\phi_3 - \phi_{exact}\rvert$	$\lvert s\psi_3 - \psi_{exact}\rvert$	$\lvert s\theta_3 - \theta_{exact}\rvert$
0.1	5.8462×10^{-8}	2.9231×10^{-8}	4.3847×10^{-8}	1.1296×10^{-9}	5.6481×10^{-10}	8.4721×10^{-10}
0.2	2.3735×10^{-7}	1.1868×10^{-7}	1.7801×10^{-7}	9.1183×10^{-9}	4.5591×10^{-9}	6.8387×10^{-9}
0.3	5.4025×10^{-7}	2.7013×10^{-7}	4.0519×10^{-7}	3.1019×10^{-8}	1.5509×10^{-8}	2.3264×10^{-8}
0.4	9.6995×10^{-7}	4.8497×10^{-7}	7.2746×10^{-7}	7.4067×10^{-8}	3.7034×10^{-8}	5.5550×10^{-8}
0.5	1.5289×10^{-6}	7.6443×10^{-7}	1.1466×10^{-6}	1.4567×10^{-7}	7.2834×10^{-8}	1.0925×10^{-7}
0.6	2.2192×10^{-6}	1.1096×10^{-6}	1.6644×10^{-6}	2.5339×10^{-7}	1.2669×10^{-7}	1.9004×10^{-7}
0.7	3.0429×10^{-6}	1.5215×10^{-6}	2.2822×10^{-6}	4.0495×10^{-7}	2.0248×10^{-7}	3.0371×10^{-7}
0.8	4.0020×10^{-6}	2.0010×10^{-6}	3.0015×10^{-6}	6.0824×10^{-7}	3.0412×10^{-7}	4.5618×10^{-7}
0.9	5.0982×10^{-6}	2.5491×10^{-6}	3.8237×10^{-6}	8.7128×10^{-7}	4.3564×10^{-7}	6.5346×10^{-7}
1	6.3334×10^{-6}	3.1667×10^{-6}	4.7500×10^{-6}	1.2023×10^{-6}	6.0113×10^{-7}	9.0170×10^{-7}

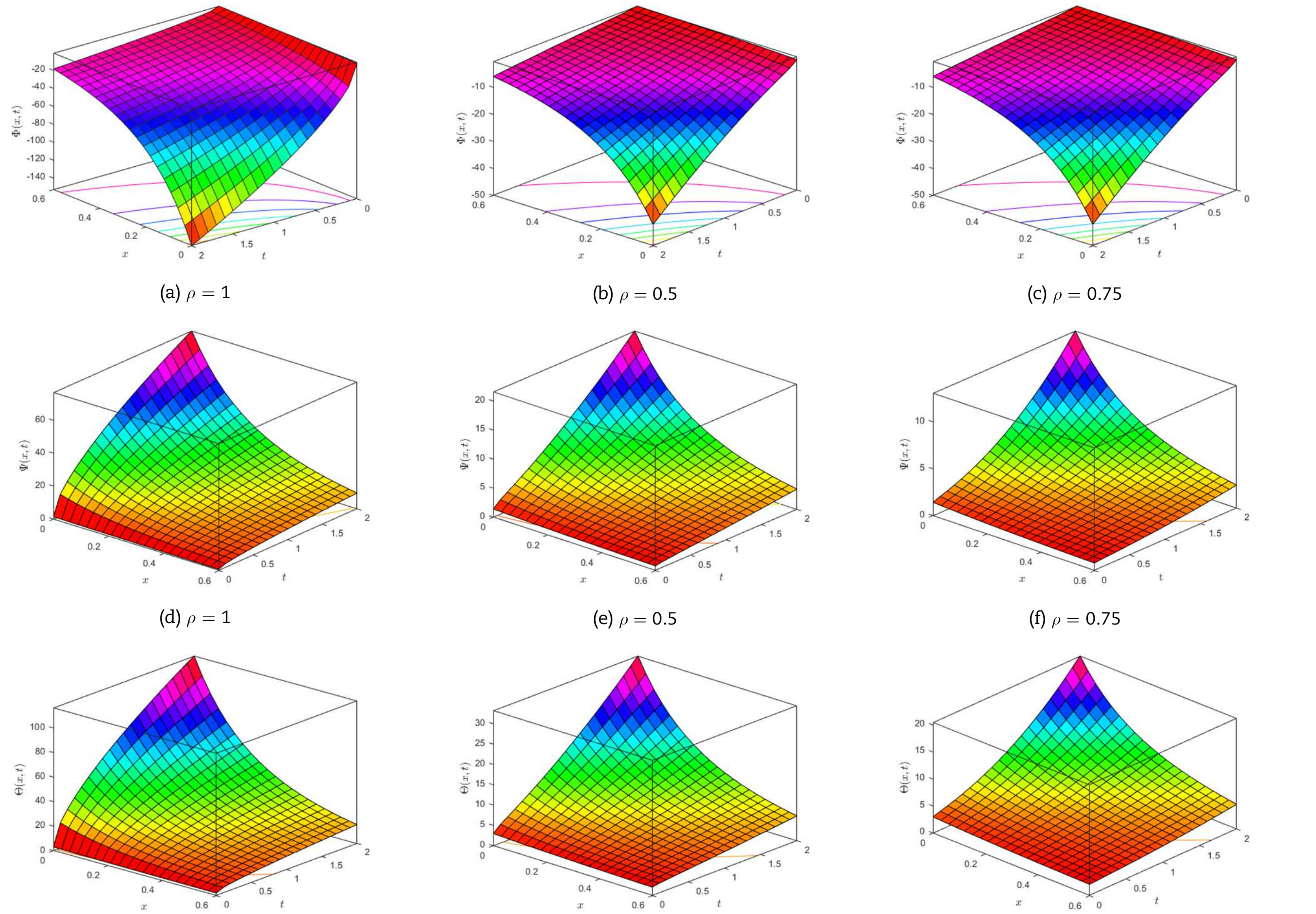

(a) $\rho = 1$ (b) $\rho = 0.5$ (c) $\rho = 0.75$

(d) $\rho = 1$ (e) $\rho = 0.5$ (f) $\rho = 0.75$

(g) $\rho = 1$ (h) $\rho = 0.5$ (i) $\rho = 0.75$

Fig. 6. Behavior of the approximate GB-HPM solution for Example 4 where (a, b, c) are for $s\phi_3$, (d, e, f) are for $s\psi_3$ and (g, h, i) are for $s\theta_3$.

6. Conclusion

In conclusion, the present study has demonstrated an efficacious two-stage method. In the first stage, the GB-transform is used to break down the temporal fractional differential operator into simpler form, after which HPM method is utilized to handle the non-linearity of the conformable time fractional non-linear KdV system. Without any modification, the GB-transform easily targets conformable fractional-order derivative as compared to published integral transforms. The conjunction of HPM with the suggested transform also eliminates the need for further linearization and discretization to efficiently solve the reduced system of differential equations. Therefore, the present scheme is capable of reducing the size of the computational labor and time. In comparison analysis, GB-HPM has surpassed the precision level of well-established methodologies such as MGMLFM, RPSM, RDTM, NDM and DTM. The graphical representation enhances the soliton dynamics of the KdV system and its variations due to the effect of fractional order. Inclusion of conformable fractional derivative contributes with enhanced view of micro deviations, bifurcations and early stages of evolutionary dynamics. Literature lacks the reliable solution in most of the cases for $0 < \rho < 1$. The closeness of consecutive approximations in terms of absolute error manifests the convergence and reliability of the obtained series solution for $0 < \rho \le 1$. It is worth noting that GB-HPM performs competently, even in the absence of an exact solution. Future research may extend with the application of GB-HPM to higher order versions of KdV equation with additional physical effects in framework of conformable space-time fractional derivative. These equations pose a significant challenge due the highly oscillatory nature. Therefore, efficient dealing with such complex systems can be a great contribution for future endeavors.

Author Contributions

Basic idea of the problem was conceived by W.X. Ma. A. Pasrija has planned the scheme and written the programs in MATLAB. S. Arora and S.S. Dhaliwal has done critical analysis. The manuscript was written through the contribution of all authors. All authors discussed the results, reviewed, and approved the final version of the manuscript.

Acknowledgments

Not applicable.

Conflict of Interest

The authors declared no potential conflicts of interest concerning the research, authorship, and publication of this article.

Funding

The authors received no financial support for the research, authorship, and publication of this article.

Data Availability Statements

The datasets generated and/or analyzed during the current study are available in the manuscript.

References

[1] Atangana, A., Baleanu, D., New fractional derivatives with non-local and non singular kernel, *Thermal Science*, 20(2), 2016, 763–769.
[2] Caputo, M., Fabrizio, M., A new definition of fractional derivative without singular kernel, *Progress in Fractional Differentiation & Applications*, 1(2), 2015, 73–85.
[3] Podlubny, I., *Fractional Differential Equations: An Introduction to Fractional Derivatives, Fractional Differential Equations, to Methods of Their Solution and Some of Their Applications*, Academic Press, USA, 1998.
[4] Diethelm, K., Garrappa, R., Giusti, A., Stynes, M., Why fractional derivatives with nonsingular kernels should not be used, *Fractional Calculus and Applied Analysis*, 23(3), 2020, 610–634.
[5] Khalil, R., Al-Horani, M., Yousef, A., Sababheh, M., A new definition of fractional derivative, *Journal of Computational and Applied Mathematics*, 264, 2014, 65–70.
[6] Abdeljawad, T., On conformable fractional calculus, *Journal of Computational and Applied Mathematics*, 279, 2015, 57–66.
[7] Atangana, A., Baleanu, D., Alsaedi, A., New properties of conformable derivative, *Open Mathematics*, 13(1), 2015, 889–898.
[8] Atangana, A., Akgül, A., Khan, M.A., Ibrahim, R.W., Conformable derivative: a derivative associated to the Riemann-Stieltjes integral, *Progress in Fractional Differentiation and Applications*, 8(2), 2022, 321–348.
[9] El-Nabulsi, R.A., Emergence of lump-like solitonic waves in Heimburg–Jackson biomembranes and nerves fractal model, *Journal of the Royal Society Interface,* 19, 2022, 20220079.
[10] El-Nabulsi, R.A. Modelling of KdV-Soliton through fractional action and emergence of lump waves. *Qualitative Theory Dynamical System,* 23(1), 2024, 298.
[11] Abdelhakim, A.A., The flaw in the conformable calculus: it is conformable because it is not fractional, *Fractional Calculus and Applied Analysis*, 22(2), 2019, 242–254.
[12] Abdelhakim, A.A., Machado, J.A.T., A critical analysis of the conformable derivative, *Nonlinear Dynamics*, 95, 2019, 3063–3073.
[13] Geyer, A., Quirchmayr, R., Shallow water equations for equatorial tsunami waves, *Philosophical Transactions of the Royal Society A: Mathematical, Physical and Engineering Sciences*, 376, 2018, 20170100.
[14] Helal, M., El-Eissa, H., Shallow water waves and Korteweg-de Vries equation (oceanographical application), *Pure Mathematics and Applications*, 7(3-4), 1996, 263–282.
[15] Kurt, A., Rezazadeh, H., Senol, M., Neirameh, A., Tasbozan, O., Eslami, M., Mirzazadeh, M., Two effective approaches for solving fractional generalized Hirota-Satsuma coupled KdV system arising in interaction of longwaves, *Journal of Ocean Engineering and Science*, 4(1), 2019, 24–32.
[16] Russell, J.S., *Report on Waves, In 14th Meeting of the British Association for the Advancement of Science*, John Murray, London, 1844, 311–390.
[17] Korteweg, D.J., De Vries, G., On the change of form of long waves advancing in a rectangular canal, and on a new type of long stationary waves, *The London, Edinburgh, and Dublin Philosophical Magazine and Journal of Science*, 39(240), 1895, 422–443.
[18] Zabusky, N.J., Kruskal, M.D., Interaction of "solitons" in a collisionless plasma and the recurrence of initial states, *Physical Review Letters*, 15(6), 1965, 240.
[19] Guo, M., Fu, C., Zhang, Y., Liu, J., Yang, H., Study of ion-acoustic solitary waves in a magnetized plasma using the three-dimensional time-space fractional Schamel-KdV equation, *Complexity*, 2018, 2018, 6852548.
[20] Lidsey, J.E., Cosmology and the Korteweg-de Vries equation, *Physical Review D*, 86(12), 2012, 123523.
[21] Kenig, C., Ponce, G., Vega, L., A bilinear estimate with applications to the KdV equation, *Journal of the American Mathematical Society*, 9(2), 1996, 573–603.
[22] Leibovich, S., Weakly non-linear waves in rotating fluids, *Journal of Fluid Mechanics*, 42(4), 1970, 803–822.
[23] Lakshmanan, M., *Solitons, Tsunamis and Oceanographical Applications of, In Encyclopedia of Complexity and Dynamical Systems, R.A. Meyers (ed.)*, Springer, New York, 2011.
[24] Wang, J., Shehzad, K., Seadawy, A.R., Arshad, M., Asmat, F., Dynamic study of multi-peak solitons and other wave solutions of new coupled KdV and new coupled Zakharov–Kuznetsov systems with their stability, *Journal of Taibah University for Science*, 17(1), 2023, 2163872.
[25] Yang, X.J., Hristov, J., Srivastava, H.M., Ahmad, B., Modelling fractal waves on shallow water surfaces via local fractional Korteweg-de Vries equation, *Abstract and Applied Analysis*, 2014, 2014, 278672.
[26] Zhang, H., Ma, W.X., Extended transformed rational function method and applications to complexiton solutions, *Applied Mathematics and Computation*, 230, 2014, 509–515.
[27] Ma, W.X., You, Y., Solving the Korteweg-de Vries equation by its bilinear form: Wronskian solutions, *Transactions of the American Mathematical Society*, 357(5), 2005, 1753–1778.
[28] Ma, W.X., Linear superposition of Wronskian rational solutions to the KdV equation, *Communications in Theoretical Physics*, 73(6), 2021, 065001.
[29] Jassim, H.K., Baleanu, D., A novel approach for Korteweg-de Vries equation of fractional order, *Journal of Applied and Computational Mechanics*, 5(2), 2019, 192–198.
[30] Ahmad, H., Khan, T.A., Stanimirovic, P.S., Ahmad, I., Modified variational iteration technique for the numerical solution of fifth order KdV-type equations, *Journal of Applied and Computational Mechanics*, 6, 2020, 1220–1227.
[31] Samad, A., Muhammad, J., Meshfree collocation method for the numerical solution of higher order KdV equation, *Journal of Applied and Computational Mechanics*, 7(2), 2021, 422–431.
[32] El-Nabulsi, R.A., A fractional model to study soliton in presence of charged space debris at low-earth orbital plasma region, *IEEE Transactions on Plasma Science*, 52(9), 2024, 4671-4693.
[33] Hirota, R., Satsuma, J., Soliton solutions of a coupled Korteweg-de Vries equation, *Physics Letters A*, 85(8-9), 1981, 407–408.
[34] Jafari, H., A new general integral transform for solving integral equations, *Journal of Advanced Research*, 32, 2021, 133–138.
[35] Elzaki, T.M., The new integral transform Elzaki transform, *Global Journal of Pure and Applied Mathematics*, 7(1), 2011, 57–64.
[36] Mohand, M., Mahgoub, A., The new integral transform 'Mohand' transform, *Advances in Theoretical and Applied Mathematics*, 12(2), 2017, 113–120.
[37] Aboodh, K.S., The new integral transform 'Aboodh' transform, *Global Journal of Pure and Applied Mathematics*, 9(1), 2013, 35–43.
[38] Khan, Z.H., Khan, W.A., N-transform-properties and applications, *NUST Journal of Engineering Sciences*, 1, 2008, 127–133.
[39] Higazy, M., Aggarwal, S., Sawi transformation for system of ordinary differential equations with application, *Ain Shams Engineering Journal*, 12(3), 2021, 3173–3182.
[40] Maitama, S., Zhao, W., New integral transform: Shehu transform a generalization of Sumudu and Laplace transform for solving differential equations, *International Journal of Analysis and Applications*, 17(2), 2019, 167–190.
[41] Yang, X.J., A new integral transform with an application in heat-transfer problem, *Thermal Science*, 20(3), 2016, 677–681.
[42] Saadeh, R., Qazza, A., Burqan, A., A new integral transform: ARA transform and its properties and applications, *Symmetry*, 12(6), 2020, 925.
[43] Saadeh, R.Z., Ghazal, B.F., A new approach on transforms: Formable integral transform and its applications, *Axioms*, 10(4), 2021, 332.
[44] Kharrat, B.N., A new integral transform: Kharrat-Toma transform and its properties, *World Applied Sciences Journal*, 38(5), 2020, 436–443.
[45] Maitama, S., Zhao, W., Beyond Sumudu transform and natural transform: J-transform properties and applications, *Journal of Applied Analysis and Computation*, 10, 2020, 1223–1241.
[46] Arora, S., Pasrija, A., A novel integral transform operator and its applications, *Iranian Journal of Numerical Analysis and Optimization*, 13(3), 2023, 553–575.

[47] Arora, S., Dhaliwal, S.S., Ma, W.X., Pasrija, A., Analysis of fractional order Schrödinger equation with singular and non-singular kernel derivatives via novel hybrid scheme, *Journal of Applied Analysis and Computation*, 15(2), 2025, 1039–1061.
[48] He, J.H., Homotopy perturbation method: A new non-linear analytical technique, *Applied Mathematics and Computation*, 135(1), 2003, 73–79.
[49] Khan, Y., Wu, Q., Homotopy perturbation transform method for nonlinear equations using He's polynomials, *Computers & Mathematics with Applications*, 61(8), 2011, 1963–1967.
[50] Roul, P., Meyer, P., Numerical solutions of systems of nonlinear integro-differential equations by homotopy-perturbation method, *Applied Mathematical Modelling*, 35(9), 2011, 4234–4242.
[51] Hetmaniok, E., Slota, D., Witula, R., Convergence and error estimation of homotopy perturbation method for Fredholm and Volterra integral equations, *Applied Mathematics and Computation*, 218(21), 2012, 10717–10725.
[52] Ghorbani, A., Beyond Adomian polynomials: He polynomials, *Chaos, Solitons & Fractals*, 39(3), 2009, 1486–1492.
[53] Alfaqeih, S., Mısırlı, E., A novel conformable Laplace transform for conformable fractional Lane–Emden type equations, *International Journal of Computer Mathematics*, 99(10), 2022, 2123–2138.
[54] Iqbal, S., Martínez, F., Kaabar, M.K., Samei, M.E., A novel Elzaki transform homotopy perturbation method for solving time-fractional non-linear partial differential equations, *Boundary Value Problems*, 2022, 2022, 91.
[55] Iqbal, S., Wang, J., Utilizing an imaginative approach to examine a fractional Newell-Whitehead-Segel equation based on the Mohand HPA, *Journal of Engineering Mathematics*, 148(1), 2024, 1–20.
[56] Al-Zhour, Z., Alrawajeh, F., Al-Mutairi, N., Alkhasawneh, R., New results on the conformable fractional Sumudu transform: theories and applications, *International Journal of Analysis and Applications*, 17(6), 2019, 1019–1033.
[57] Al-Zhour, Z., Al-Mutairi, N., Alrawajeh, F., Alkhasawneh, R., New theoretical results and applications on conformable fractional natural transform, *Ain Shams Engineering Journal*, 12(1), 2021, 927–933.
[58] Ali, H.M., An efficient approximate-analytical method to solve time-fractional KdV and KdVB equations, *Information Science Letter*, 9(3), 2020, 189–198.
[59] Senol, M., Ayse, A., Approximate solution of time-fractional KdV equations by residual power series method, *Balıkesir Üniversitesi Fen Bilimleri Enstitüsü Dergisi*, 20(1), 2018, 430–439.
[60] Keskin, Y., Oturanc, G., Reduced differential transform method for generalized KdV equations, *Mathematical and Computational Applications*, 15(3), 2010, 382–393.
[61] Saha Ray, S., Numerical solutions and solitary wave solutions of fractional KdV equations using modified fractional reduced differential transform method, *Computational Mathematics and Mathematical Physics*, 53(12), 2013, 1870–1881.
[62] Elbadri, M., Ahmed, S.A., Abdalla, Y.T., Hdidi, W., A new solution of time fractional coupled KdV equation by using natural decomposition method, *Abstract and Applied Analysis*, 2020, 2020, 3950816.
[63] Liu, J.C., Hou, G.L., New approximate solution for time-fractional coupled KdV equations by generalised differential transform method, *Chinese Physics B*, 19(11), 2010, 110203.

ORCID iD

Shelly Arora https://orcid.org/0000-0002-2817-7049
Wen Xiu Ma https://orcid.org/0000-0001-5309-1493
Sukhjit Singh Dhaliwal https://orcid.org/0000-0002-2039-492X
Atul Pasrija https://orcid.org/0009-0006-4345-5074

How to cite this article: Arora S., et al., Semi-Analytic Scheme for Fractional Insight into Multi-Component KdV System Arises in Water Wave Mechanism, *J. Appl. Comput. Mech.*, 12(2), 2026, 632-647. https://doi.org/10.22055/jacm.2025.48506.5285